Chemistry & Biology
Article

Synaptic MAGUK Multimer Formation Is Mediated by PDZ Domains and Promoted by Ligand Binding

Nils Rademacher,[1] Stella-Amrei Kunde,[1] Vera M. Kalscheuer,[2] and Sarah A. Shoichet[1,*]
[1]Neuroscience Research Center and Cluster of Excellence NeuroCure, Charité-Universitätsmedizin, 10117 Berlin, Germany
[2]Max Planck Institute for Molecular Genetics, 14195 Berlin, Germany
*Correspondence: sarah.shoichet@charite.de
http://dx.doi.org/10.1016/j.chembiol.2013.06.016

SUMMARY

To examine the scaffolding properties of PSD-95, we have taken advantage of established ligand/PDZ domain interactions and developed a cell-based assay for investigating protein complex formation. This assay enables quantitative analysis of PDZ domain-mediated protein clustering using bimolecular fluorescence complementation (BiFC). Two nonfluorescent halves of EYFP were fused to C-terminal PDZ ligand sequences to generate probes that sense for PDZ domain binding grooves of adjacent (interacting) molecules. When these probes are brought into proximity by the PDZ domains of a multiprotein scaffold, a functional fluorescent EYFP molecule can be detected. We have used this system to examine the properties of selected PSD-95 variants and thereby delineated regions of importance for PSD-95 complex formation. Further analysis led to the finding that PSD-95 multimerization is PDZ domain-mediated and promoted by ligand binding.

INTRODUCTION

The postsynaptic density (PSD) of excitatory synapses is a highly organized structure consisting of multiple densely packed interacting proteins (for reviews see Sheng and Hoogenraad, 2007 and Okabe, 2007). Members of the membrane-associated guanylate kinase (MAGUK) family, together with other scaffold proteins at the PSD, provide a structural framework for protein complex formation, thereby serving as regulatory hubs that enable efficient regulation of synaptic signal transduction (Funke et al., 2005; Good et al., 2011). These scaffold proteins typically contain a series of modular protein interaction domains enabling them to locally cluster various target proteins. In this study, we focus on PSD-95, which is arguably the most abundant PDZ domain scaffold protein in the postsynaptic density (Cheng et al., 2006). PSD-95 plays an important role in the incorporation of AMPA receptors into the postsynapse upon induction of long-term potentiation (LTP) (Ehrlich and Malinow, 2004; Zhang and Lisman, 2012), which presumably underlies its essential role in learning and memory. PSD-95 consists of three PDZ domains followed by a src homology 3 (SH3) domain and a guanylate kinase-like (GK) domain (Cho et al., 1992). PDZ domains 1 and 2 of PSD-95 bind to various membrane proteins including the NMDA receptor subunits (Kornau et al., 1995), whereas the third PDZ domain of PSD-95 (PDZ3) preferentially binds the C termini of a different set of proteins, including, for example, the synaptic protein CRIPT (Niethammer et al., 1998).

Several mechanisms of protein clustering via PSD-95 multimerization have been put forward: a "head-to-head" configuration of PSD-95 molecules through covalent linkage of two N-terminal cysteines (Cys 3 and Cys 5) has been described (Hsueh et al., 1997) (Hsueh and Sheng, 1999). Other studies have shown that these two cysteines can be reversibly palmitoylated (El-Husseini et al., 2000), leading to an enrichment of PSD-95 molecules at the synaptic membrane (Christopherson et al., 2003; El-Husseini et al., 2002). A theoretical tail-to-tail association of PSD-95 molecules by an intermolecular interaction between SH3-GK modules has also been proposed (McGee et al., 2001). Of special relevance for this study is a recent finding that as many as 30% of known mammalian PDZ domains may interact directly with other PDZ domains (Chang et al., 2011).

We are interested in exploring how the PDZ domains of multiprotein complexes like those comprising the PSD are arranged and regulated and have developed an assay that is sensitive to nanoscale rearrangements of PSD-95 PDZ binding grooves and enables investigation of PSD-95 complex formation in a cellular context. This clustering assay relies on bimolecular fluorescence complementation (Ghosh et al., 2000; Kerppola, 2006) and takes advantage of the well-characterized interaction between specific PDZ domains and their ligand C termini. By fusing nonfluorescing halves of enhanced yellow fluorescent protein (EYFP) to the C-terminal sequences of known PDZ ligands, we have generated tools that allow us to monitor the proximity of PDZ domains via observation of reassembled EYFP, and with these tools, we demonstrate that PDZ domains of neighboring PSD-95 molecules come into close contact with one another. By further analysis of the underlying mechanism, we provide evidence that multimerization of PSD-95 molecules is mediated by ligand binding to PDZ domains.

RESULTS

PDZ Ligand C Termini Fused to Split-EYFP Fragments Are Clustered by PSD-95

In order to monitor the ability of PDZ domain proteins to bring their PDZ ligand binding partners into close proximity, we fused

nonfluorescing (N-terminal and C-terminal) EYFP fragments to known PDZ domain-binding sequences (Figure 1A); upon transfection of both halves together with a PDZ domain protein such as PSD-95, fluorescence is observed. More specifically, we fused the ten C-terminal amino acids (DTKNYKQTSV) of CRIPT, a cytosolic neuronal protein that has been shown to interact with PSD-95 via its C-terminal end in a classical ligand-PDZ domain interaction, to the C-terminal ends of both nonfluorescing EYFP halves. To allow for some flexibility, we inserted a 15 amino acid flexible linker sequence, composed of serial glycines and serines (3× GGGGS), between the EYFP and CRIPT sequences. We thus generated split-EYFP PDZ probes that in theory, like CRIPT, bind preferentially to PDZ3 and with reduced affinity to other PDZ domains in PSD-95 (Lim et al., 2002; Niethammer et al., 1998) and can thereby be used to assess the ability of PSD-95 molecules to form complexes in which the PDZ domain regions are in close proximity. In order to form a fluorescent molecule, the two nonfluorescent halves of EYFP must come into direct contact with one another. Based on the sequence of our linker, the maximum distance between an EYFP half and the ten amino acid C terminus is ~5 nm; our system therefore serves as a readout for ligand clustering by closely neighboring PDZ domains, which we examine in the context of a cell-based assay by making use of a series of tagged PSD-95 variants and split-EYFP PDZ probes (depicted in Figure 2). In the context of this assay, effective ligand clustering results in increased EYFP refolding.

To rule out the possibility that either of the two split-EYFP fragments was able to generate a fluorescence signal on its own, we overexpressed PSD-95 with each split-EYFP half independently. Significant fluorescence, observable in the cytoplasm by live-cell fluorescence imaging of EYFP (Figure 1B) is indeed observed only in the presence of both split halves (comparison done by flow cytometry, Figure 1C; see Figure 1D for quantification). A control western blot (Figure 1E) confirms expected levels of overexpressed proteins following transfections done in parallel to those used for the flow cytometric analysis shown in Figure 1D. We also confirmed that significant clustering of split-EYFP halves requires the presence of a scaffold-competent PDZ domain protein by exchanging PSD-95 with either the red fluorescent protein mCherry or the isolated PSD-95 SH3-GK module for comparison (Figure 1F). When expressed in the absence of a third protein, overexpression of both split-EYFP halves results in a somewhat higher background signal (see Figure S1A available online), presumably reflecting the nonspecific effects of comparing double versus triple transfections. We likewise observe that EYFP refolding reflects, to some extent, the quantity of EYFP halves used in the assay (see Figure S1B, top panel) and therefore adhere to selected transfection conditions (50 ng each split-EYFP half plus 300 ng scaffold protein per transfection) for subsequent comparative experiments. Importantly, our signal clearly reflects a clustering process that occurs efficiently with specificity for selected proteins.

Clustering of Split-EYFP PDZ Probes Depends on Ligand-PDZ Domain Interactions

Subsequent experiments involved a series of mutants that were designed for further validation of specificity. First we confirmed that reassembly of split-EYFP PDZ probes definitively relies on the intact interaction between PDZ domains and C-terminal ligand sequences. By substituting anchor residues at position 0 and −2 in the C-terminal CRIPT sequence (QTSV → QASA; see Figure 2 for schematic depiction of variants), the ligand-PDZ domain interaction is disrupted: when split-EYFP halves are fused to CRIPT C-terminal sequences that are mutated in this way (referred to throughout the text as YN- or YC-CRIPT-mut), we observe dramatically reduced EYFP fluorescence in our clustering assay with PSD-95 (Figure 3A, left panel; see Figure S1B, upper panel for titration). This result is supported by coimmunoprecipitation (coIP) experiments where we observe a corresponding abolished binding to PSD-95 by the mutant ligand (compare Figures S2Ai and S2Aii).

The interaction between the CRIPT C terminus and PSD-95 also depends on the integrity of the PDZ domains within PSD-95. In order to verify that this is also reflected in our split-EYFP system, we generated PDZ domain mutants as previously described (Doyle et al., 1996; Regalado et al., 2006; Zheng et al., 2010), by substituting conserved phenylalanine residues in the carboxylate binding loop (GLGF) with histidine (F → H; PSD-95 PDZmut, see schematic in Figure 2; see also Experimental Procedures for detailed description). Such PDZ domain modifications are expected to hinder the interaction between overexpressed PSD-95 and CRIPT split-EYFP PDZ probes; we do, however, observe some binding by coIP (Figures S2Aiii and S2Biii). Importantly, we observe reduced fluorescence in our clustering assay with this mutant protein relative to the wild-type PSD-95 (Figure 3A middle panel; see Figure S1B, middle panel for titration) despite comparable protein expression levels (controlled by western blot, data not shown). Taken together, these data indicate that our assay detects PSD-95-mediated clustering of PDZ probes and that the fluorescence signal relies on the interaction between the ligand C-terminal sequence and a partner PDZ domain. When this interaction is intact, we can thus use this system to investigate how other modifications affect the ability of PSD-95 to mediate ligand clustering.

Site-Directed Mutagenesis Highlights Residues within PSD-95 That Are Important for Clustering

The C-terminal SH3-GK module of PDS-95 family molecules exists substantially in a folded state (McGee et al., 2001; Tavares et al., 2001), and several specific residues within this region are critical for maintaining the intramolecular interaction between the SH3 and GK domains that is necessary for normal scaffolding and function of the full-length protein. We have taken advantage of a previously described point mutation (L460P) in the SH3-GK module of PSD-95, which has been shown to disrupt this intramolecular SH3-GK association (McGee and Bredt, 1999; Shin et al., 2000) and channel clustering (Shin et al., 2000). With regard to protein levels, this mutant behaved like the wild-type following heterologous expression (Figure S3); however, it was unable to cluster the CRIPT split-EYFP PDZ probes like the wild-type PSD-95 (Figure 3A, right panel; see Figure S1B, lower panel for titration). Importantly, this point mutation did not abolish binding of PSD-95 to its split-EYFP ligand binding partners in coIP experiments (Figure S2Aiv), which suggests that—despite conformational changes within the C-terminal half of the protein—the PDZ domain binding groove "slots" in

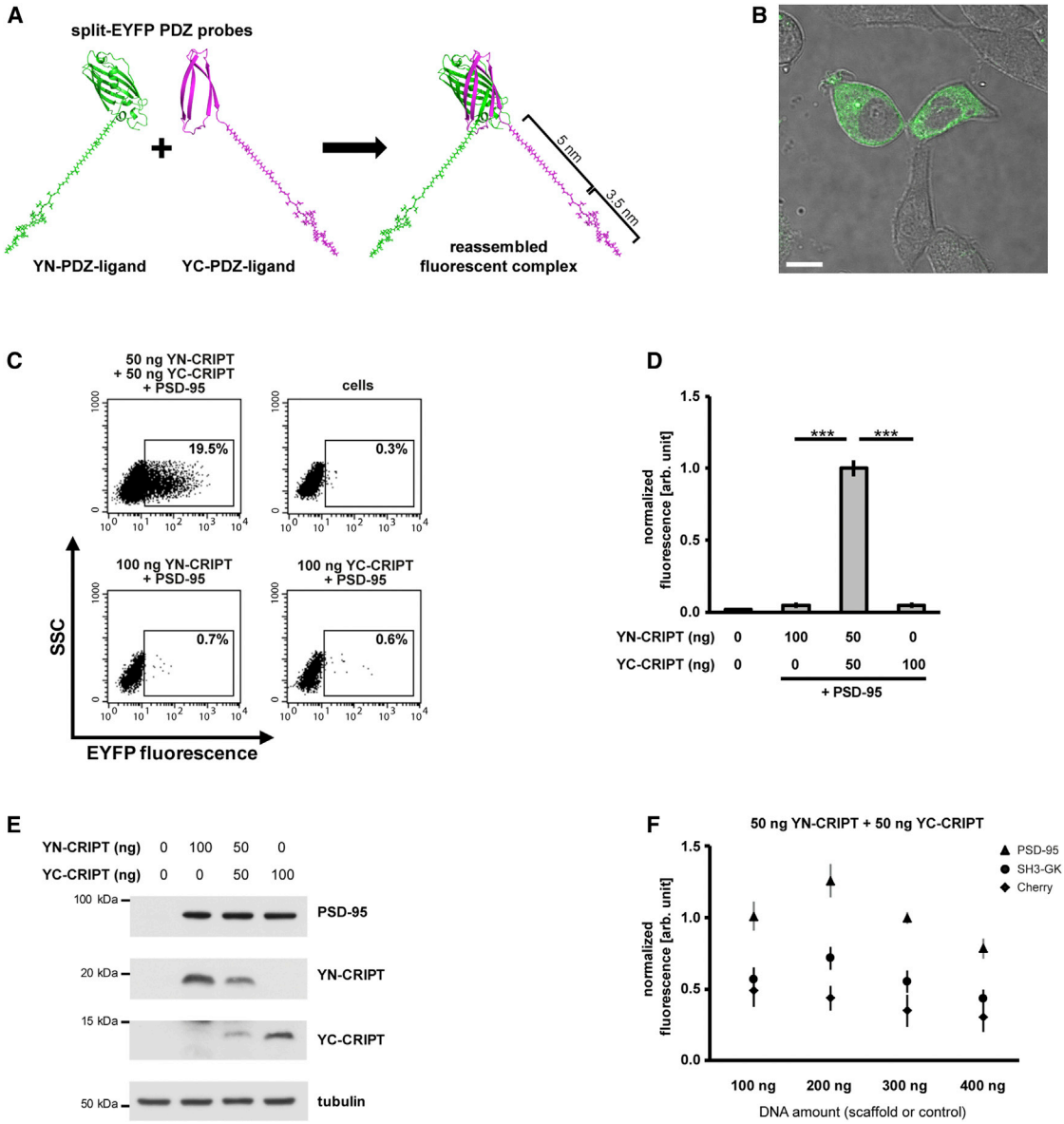

Figure 1. PDZ Ligand C Termini Fused to Split-EYFP Fragments Serve as Probes for PSD-95 PDZ Domains

(A) Nonfluorescent N-terminal (YN, amino acids 1–154) and C-terminal (YC, amino acids 155–238) fragments of EYFP were fused to flexible 15 amino acid (3× GGGGS) linkers (~5 nm), followed by ten C-terminal amino acids of a known PDZ ligand (~3.5 nm). The resulting constructs (YN-PDZ-ligand and YC-PDZ-ligand) are referred to as "PDZ probes" throughout this study. Upon binding to closely neighboring PDZ domains, the two split-EYFP PDZ probes are brought into close proximity, enabling reassembly of the EYFP halves to form a fluorescent complex.

(B) Live-cell microscopy of COS-7 cells transfected with PSD-95 (300 ng) and CRIPT split-EYFP probes (50 ng each half). Scale bar indicates 10 μM.

(C) Representative example of quantitative assay readout by flow cytometry. Dot plots of single flow cytometric measurements of COS-7 cells transfected with different split-EYFP PDZ probe (YN-CRIPT and/or YC-CRIPT)/PSD-95 combinations. Each dot plot represents 10,000 cells.

(D) Bar diagram of a flow cytometry-based clustering assay with construct combinations as shown in (B). Each bar represents flow cytometric measurements of four independent experiments performed in triplicate (each bar contains information from 12 × 10,000 cells). Formation of a fluorescent complex is based on the presence of both split-EYFP PDZ probe halves. Data were analyzed with 1-way ANOVA/Bonferroni multiple comparison test; bars represent mean values ± SD. ***$p < 0.001$.

(E) Representative western blot serves as protein expression control for a single experiment (comparable to one of the four experiments summarized in C). Each lane contains protein from pooled triplicates. PSD-95 is detected with αFLAG antibody (rabbit). YN-CRIPT and YC-CRIPT are detected with αGFP antibody (goat). Protein size marker positions are indicated.

(F) Clustering assay: coexpressing a fixed DNA amount of CRIPT split-EYFP probes (50 ng each half) together with different DNA amounts of PSD-95, SH3-GK, and mCherry. Data points reflect mean values from four independent experiments each done in triplicate; error bars indicate SD. Efficient clustering is only observed if a PDZ domain protein is coexpressed.

See also Figure S1A.

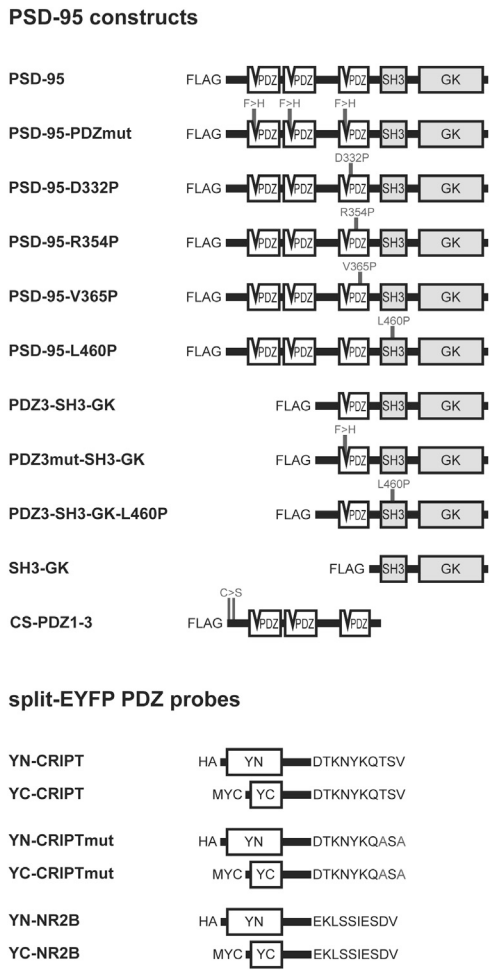

Figure 2. Schematic Representations of PSD-95-Derived Expression Constructs and Split-EYFP PDZ Probes Used in This Study

All PSD-95 constructs harbor N-terminal FLAG tags. Protein domains and targeted amino acid exchanges (F > H, D332P, R354P, V365P, L460P, C > S) are indicated. YN and YC refer to N- and C-terminal halves of EYFP as depicted in Figure 1A. All PDZ probes are additionally tagged with N-terminal Myc or HA tags as indicated.

PSD-95 remain available for ligand binding. This result indicates that our reassembled EYFP signal relies not only on the proper binding of the C-terminal ligand sequence to its partner PDZ domain, but also on the integrity of the SH3-GK module.

In order to identify other residues that interfere with PSD-95 complex assembly, we used this platform to screen several additional point mutations within the context of the full-length protein (including residues S73 [Steiner et al., 2008], S295 [Kim et al., 2007], Y397 [Pan et al., 2011], R568 [Reese et al., 2007], D332, R354, and V365 [Reynolds et al., 2011], among others). A single additional mutant (R354P), one of three mutants tested that affect surface regions of the PDZ3 domain that are distinct from the ligand binding groove (see Figure 3B), yielded a significantly reduced clustering signal when compared to the wild-type PSD-95 (Figure 3C). Like the L460P mutant tested previously, which effects the SH3-GK domain, this PSD-95-R354P mutant also maintained its ability to bind CRIPT split-EYFP PDZ probes (data not shown); thus, our results suggest that selected residues within the third PDZ domain might also affect global PSD-95 protein integrity in a way that influences complex assembly.

Intramolecular Ligand Clustering versus PSD-95 Multimer Formation

If we modify this assay and exchange the CRIPT C termini, which bind preferentially to PDZ3, for C-terminal sequences of the NMDA receptor subunit NR2B, which bind preferentially to PDZ1 and also to PDZ2 of PSD-95 (Lim et al., 2002) (see schematic diagram, Figure 4A), we observe increased clustering (Figure 4B). It is likely that observed fluorescence with NR2B split-EYFP PDZ probes reflect a combination of ligand clustering mediated by PSD-95 multimer formation (i.e., probes bind to different interacting scaffold molecules) and ligand clustering by single PSD-95 molecules (where two probes bind to one PSD-95 molecule). Given that PSD-95 is known to form multimers (Christopherson et al., 2003; Hsueh et al., 1997; McGee et al., 2001), together with the fact that a point mutation affecting the function of the SH3-GK module of PSD-95 (L460P) is not able to effectively cluster CRIPT split-EYFP PDZ probes despite efficient binding to them, we propose that our CRIPT-mediated fluorescence signal predominantly reflects that PSD-95 complex formation forces PDZ domains from neighboring molecules into close proximity. We are interested in particular in ligand clustering that is mediated by such multimeric scaffold formation; we have therefore designed subsequent experiments in order to investigate how PSD-95 variants influence this process.

Distinct Subdomains of PSD-95 Are Sufficient for Clustering PDZ Probes

We generated a mutant PSD-95 construct that consists only of the MAGUK core domains (PDZ3-SH3-GK) (Anderson, 1996), and in the same CRIPT-mediated bimolecular fluorescence complementation (BiFC) assay, this short form of PSD-95 was also able to cluster CRIPT split-EYFP PDZ probes, albeit somewhat less efficiently than the wild-type PSD-95 (see Figure 4C for comparison). Compared to probes harboring the mutated C-terminal CRIPT sequence, wild-type CRIPT probes reassembled with ~3-fold efficiency in the presence of PDZ3-SH3-GK construct, indicating that this truncated PSD-95 protein is also able to promote the availability of closely neighboring PDZ slots for ligand binding. Given that each PDZ3-SH3-GK molecule has only one ligand-binding PDZ domain, this likely occurs via the formation of complexes that harbor multiple PDZ3-SH3-GK molecules, i.e., this result confirms our hypothesis that we can use this assay to assess PDZ protein complex formation. We next investigated this multimolecular clustering by PDZ3-SH3-GK using mutant proteins corresponding to those used in the initial set of experiments with the full-length PSD-95 constructs. Similar to the case of the full-length protein, if we generate a point mutation in the ligand binding groove of the PDZ domain of PDZ3-SH3-GK (PDZ3mut-SH3-GK), we decreased reassembly of CRIPT split-EYFP PDZ probes (Figure 5A), and as we observed for the wild-type PSD-95, the interaction of this short PSD-95 variant with the CRIPT split-EYFP PDZ probes also requires an intact ligand C-terminal sequence (compare Figures S2Bi and S2Bii). Interestingly, CRIPT PDZ probes maintain some ability to bind to the PDZ3mut-SH3-GK harboring the

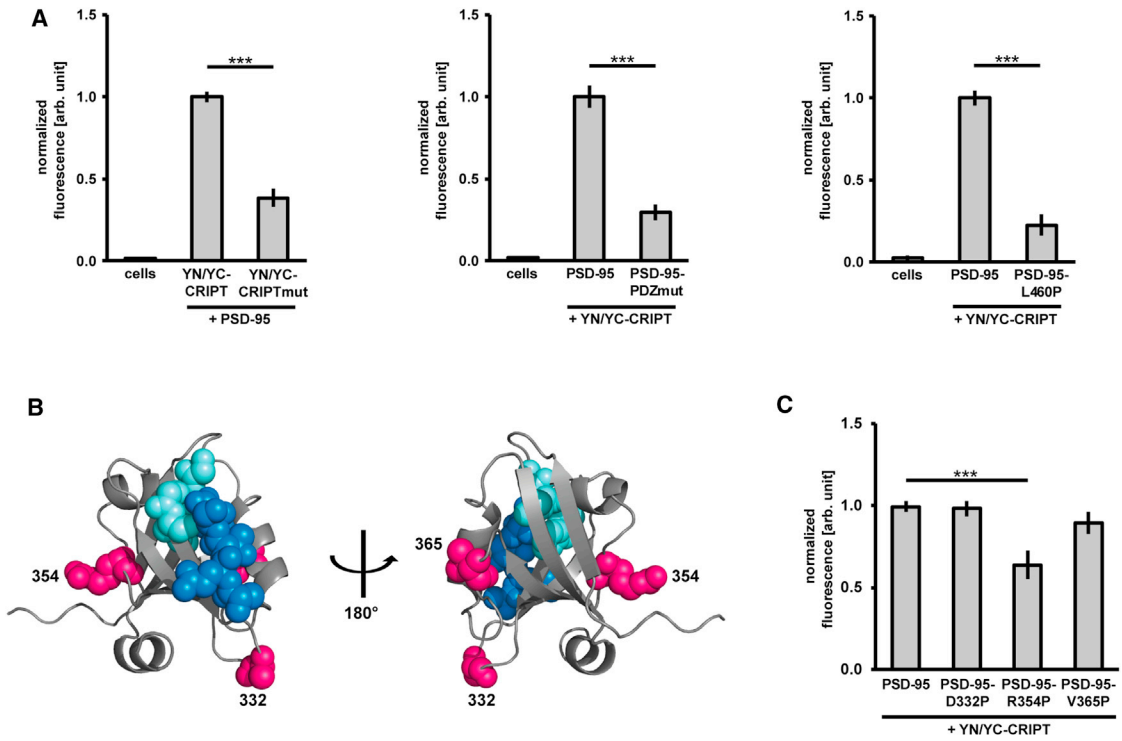

Figure 3. Clustering of Split-EYFP PDZ Probes by PSD-95 Variants

Bar diagrams of flow cytometry-based clustering assays comparing normalized fluorescence intensity after expression of different combinations of PSD-95 and CRIPT split-EYFP PDZ probe variants.

(A) Left: Clustering assay with PSD-95 and CRIPT split-EYFP PDZ probes (with C-terminal CRIPT amino acid sequence DTKNYKQTSV) or CRIPTmut split-EYFP PDZ probes (with C-terminal CRIPTmut amino acid sequence DTKNYKQ**ASA**). Site-directed mutagenesis of two anchor residues (positions 0 and −2) to alanines within the C-terminal PDZ ligand reduces CRIPT split-EYFP PDZ probe clustering by PSD-95. Middle: Clustering of CRIPT split-EYFP PDZ probes by PSD-95 or PSD-95-PDZmut (triple PDZ domain mutant F77H, F172H, F325H). Site-directed mutagenesis of the conserved phenylalanines in the central carboxylate binding loops GLG**F**) of PSD-95 PDZ domains to histidines leads to a reduced clustering of split-EYFP probes. Right panel: Clustering of CRIPT split-EYFP PDZ probes by PSD-95 or PSD-95-L460P. Site-directed mutagenesis of leucine 460 in the SH3 domain to proline reduces clustering activity. Two-tailed unpaired t tests, mean values ± SD. ***$p < 0.001$, each bar graph represents summary of four times triplicate experiments, as described for Figure 1D. See also Figures S1B, S2, and S3.

(B) PSD-95 PDZ3 surface residues were tested for their ability to influence PDZ probe clustering. Model of the third PDZ domain of PSD-95 bound to a CRIPT-derived peptide (based on the Protein Data Bank [PDB] file 1BE9, generated in PyMOL). The GLGF motif (integral for peptide binding) is shown in cyan, the peptide (KQTSV) is shown in blue, and the three tested surface residues D332, R354, and V365 are shown in pink. Note that the three tested residues are located distal to the peptide binding groove and have no direct contact to the peptide.

(C) Bar diagram of a clustering assay comparing CRIPT split-EYFP PDZ probe clustering by PSD-95 and PSD-95 PDZ3 mutants. One-way ANOVA/Bonferroni multiple comparison test, mean values ± SD. ***$p < 0.001$. Each bar graph represents a summary of four times triplicate experiments, as described for Figure 1D.

PDZ domain point mutation (Figure S2Biii). Importantly, when we mutate the SH3-GK module as we did in the full-length L460P construct (to generate PDZ3-SH3-GK-L460P) we again abolish reassembly of CRIPT split-EYFP PDZ probes (Figure 5A) without disrupting the interaction between the ligand and the PDZ domain (Figure S2Biv). In summary, this short variant of PSD-95, which has only one ligand-binding slot, is able to promote ligand clustering, and this process is likewise disrupted by altering the SH3-GK module structure. Together these data confirm that our refolded EYFP signal indeed reflects multiprotein complex formation and affirms the idea that SH3-GK module integrity influences this multimolecular PSD-95 scaffolding.

Interestingly, deletion constructs lacking the entire SH3-GK module are also capable of clustering the CRIPT split-EYFP PDZ probes. The distal N-terminal region, specifically via palmitoylation of two cysteine residues (C3, C5), has previously been implicated in both synaptic targeting and PSD-95 multimer formation (Christopherson et al., 2003; El-Husseini et al., 2002). We show that this N-terminal region, together with the three PDZ domains of PSD-95, is able to promote reassembly of CRIPT split-EYFP PDZ probes, even when these critical cysteine residues have been exchanged to serines (Figure S4, CS-PDZ1-3). Given that observed fluorescence at least partially reflects multimolecular scaffolding (as indicated by our clustering data using PSD-95 variants harboring a single PDZ domain, see Figures 4C and 5A), this result suggests that the isolated PDZ region of PSD-95 might also be involved in PSD-95 complex formation. We next pursued this idea using a different strategy.

PSD-95 Homotypic Multimerization Is PDZ Domain-Mediated and Requires Ligand Binding

We investigated PSD-95 multimerization via coimmunoprecipitation studies using wild-type PSD-95 and PSD-95 variants. In initial experiments, we observed, at most, a weak interaction

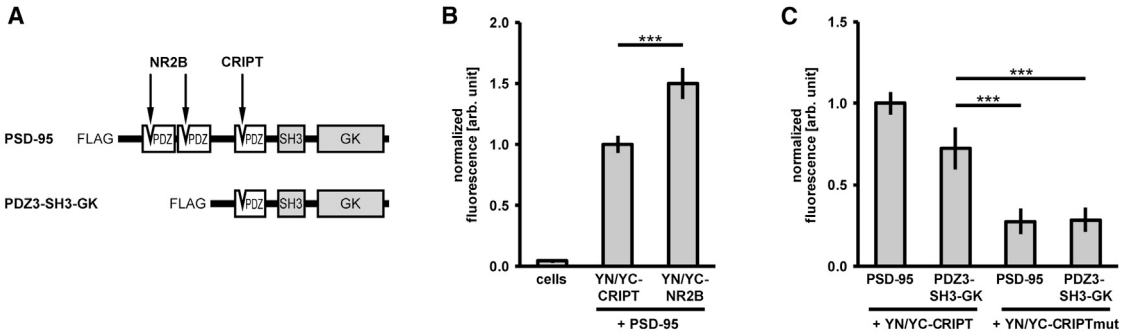

Figure 4. Intramolecular Probe Clustering versus PSD-95 Multimer Formation

(A) Schematic representation of C-terminal PDZ ligand binding preferences for specific PSD-95 PDZ domains.

(B) Normalized green fluorescence as a measure of either intramolecular ligand clustering or PSD-95 multimer formation: Clustering assay with PSD-95 and either CRIPT split-EYFP PDZ probes (that preferentially bind PDZ3) or NR2B split-EYFP PDZ probes (that preferentially bind PDZ2 and also PDZ1). Two-tailed unpaired t test, mean values ± SD. ***$p < 0.001$.

(C) Comparison of CRIPT split-EYFP PDZ probe clustering by PDZ3-SH3-GK (PSD-95 variant scaffold protein harboring one PDZ domain) with PSD-95 (PDZ scaffold protein harboring three PDZ domains). One-way ANOVA/Bonferroni multiple comparison test, mean values ± SD. ***$p < 0.001$. In (B) and (C) each bar graph represents summary of four times triplicate experiments, as described for Figure 1D.

See also Figures S2 and S3.

between differentially tagged wild-type PSD-95 molecules (data not shown), in line with previous studies indicating that isolated PSD-95 is a monomer (Fomina et al., 2011; McCann et al., 2012; Nakagawa et al., 2004). This highlights the importance of endogenous interactors and/or posttranslational modifications in this multimerization process. Interestingly, we observe that the interaction between wild-type forms of PSD-95 can be facilitated by the presence of PDZ-binding ligand sequences. More specifically, when we coexpress differentially tagged PSD-95 constructs together with CRIPT C termini (ten amino acids: DTKNYKQTSV, tagged with the monomeric red fluorescent protein mCherry at the N terminus), an interaction between PSD-95 molecules is promoted (Figure 5B, MYC-IP second lane). Importantly, this effect is not observed in the presence of comparable non-PDZ binding mutants (mCherry-tagged CRIPT C termini with alanine substitutions at positions 0 and −2: CRIPTmut; Figure 5B, MYC-IP third lane). In order to exclude the possibility that the mCherry-tagged CRIPT C termini themselves form multimeric complexes and thereby link PSD-95 molecules to each other indirectly (thus mimicking PSD-95 protein multimerization), we additionally tested for interactions between PSD-95 and other proteins that are known to interact with the CRIPT C terminus, in similar coIP assays. Such ligand-dependent "bridging" was not observed (data not shown), ruling out the possibility that the observed PSD-95 multimerization simply results from unexpected multimer formation of the mCherry-tagged CRIPT C termini. We also confirmed that the MYC antibody does not immunoprecipitate the FLAG-tagged proteins in the absence of MYC-tagged PSD-95 (Figure 5B, MYC-IP first lane), further validating the specificity of this method to answer our questions on PSD-95 multimerization. Importantly, our result suggests that the formation of PSD-95 multimers is influenced by ligand binding to partner PDZ domains. To investigate this idea further, we compared the ability of wild-type PSD-95 to interact with diverse PSD-95 variants in the presence of either wild-type or mutant mCherry-tagged CRIPT C termini, and we consistently found that interactions with the wild-type PSD-95 in this assay were dramatically enhanced by the presence of PDZ-binding ligand sequences (for all constructs with intact PDZ domains). Specifically, we observe a comparably weak interaction between PSD-95 and the SH3-GK module (SH3-GK, construct depicted in Figure 2), regardless of whether an intact or mutant CRIPT sequence is present (Figure 5Ci). Likewise, the interaction between PSD-95 and PSD-95-PDZmut is comparably weak, regardless of whether CRIPT or CRIPTmut is present (Figure 5Cii). However, the interaction between PSD-95 and the short PSD-95 variant (PDZ3-SH3-GK) is much stronger in the presence of the PDZ-binding-competent CRIPT sequence relative to that observed when the mutant CRIPT construct (CRIPTmut) is present (Figure 5Ciii), and the same result is observed when we test for self-association of PDZ3-SH3-GK in comparable assays (data not shown). This also applies for the case of the palmitoylation-deficient PSD-95 variant harboring only the three PDZ domains (CS-PDZ1-3, Figure 5Civ). Taken together, these data provide substantial evidence for a positive correlation between PDZ-ligand interactions and PSD-95 multimerization.

DISCUSSION

In summary, we have designed a strategy for detecting the presence of neighboring PDZ slots in a multimeric PSD-95 complex. Our assay relies on the sequence-specific interaction of recombinant split-EYFP PDZ probes with their partner PDZ domains. Using these probes, we demonstrate that PDZ domains of neighboring wild-type PSD-95 molecules come into close proximity of one another, whereas mutations that disrupt the structural integrity of the PSD-95 molecule are capable of preventing this type of PSD-95 protein complex formation. With these tools, we are equipped to screen PSD-95 and related proteins for regions and residues that influence scaffold complex formation, and our data illustrate the utility of the assay for this purpose. For example, the effects of the previously described L460P mutation on the structure of the SH3-GK module and the nature of the

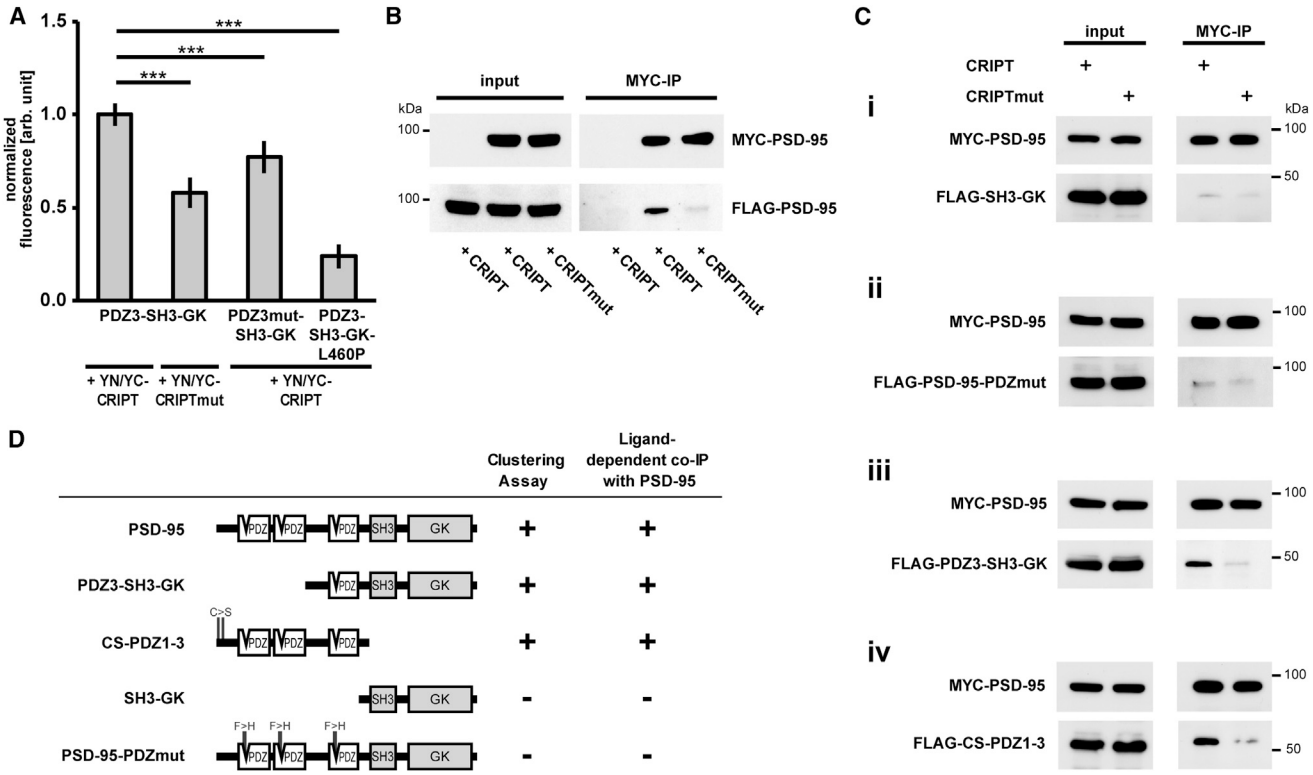

Figure 5. PDZ Ligand Clustering by PSD-95 Multimerization

(A) Clustering of CRIPT split-EYFP PDZ probes with single PDZ domain scaffold proteins (as measured by normalized fluorescence intensity following transfection of variants). Bar graphs represent summary of four times triplicate experiments; in this diagram CRIPT split-EYFP PDZ probe clustering by PDZ3-SH3-GK serves as the internal standard (with one-way ANOVA/Bonferroni multiple comparison test, mean values ± SD. ***$p < 0.001$).

(B) PSD-95 multimerization is PDZ domain-mediated and requires a PDZ ligand: following coexpression of MYC-PSD-95 with or without FLAG-PSD-95, together with mCherry-tagged wild-type or mutant CRIPT C-terminal amino acids (CRIPT and CRIPTmut), proteins were immunoprecipitated from the cell lysates with αMYC-antibody and detected by western blot. Lysate (Input) control is on the left. Coexpression of the wild-type CRIPT C terminus markedly enhanced PSD-95-PSD-95 interaction (PSD-95 multimerization). Protein size markers are indicated. CRIPT and CRIPTmut C-terminal sequences are identical to the C termini of the split-EYFP PDZ probes depicted in Figure 2.

(C) Following coexpression of MYC-PSD-95 and FLAG-tagged PSD-95 variants together with either mCherry-tagged CRIPT or mCherry-tagged CRIPTmut C termini, PSD-95 was immunoprecipitated with αMYC-antibody, and coimmunoprecipitated proteins were analyzed by western blot with FLAG antibodies (as indicated on the left). Coexpression of the wild-type CRIPT C terminus enhanced the coIP of PDZ3-SH3-GK (iii) and CS-PDZ1-3 (iv) with MYC-PSD-95, whereas coIP of SH3-GK (i) or PSD-95-PDZmut (ii) with MYC-PSD-95 was negligible regardless of whether or not the wild-type CRIPT C terminus was present.

(D) Summary of PSD-95-derived expression constructs concerning their ability to cluster CRIPT split-EYFP PDZ probes and to coimmunoprecipitate with wild-type PSD-95 in a PDZ ligand-dependent manner.

See also Figures S2, S3, and S4.

PSD-95 molecule self-association (McGee et al., 2001; Shin et al., 2000) are apparent using our bimolecular fluorescence complementation assay as a readout. Despite the presence of intact PDZ domains that are capable of interaction with ligand C termini, this mutant is unable to effectively generate a platform for positioning our split-EYFP tagged CRIPT C termini next to each other; protein-protein interactions promoted by this structural mutant clearly prevent PDZ3 domains from coming into close contact with one another. We also show that a specific PDZ3 point mutant that does not directly target the binding groove, namely the R354P mutation on the distal side of the PDZ3 domain, is able to influence ligand clustering, and this occurs without disrupting the interaction between the PDZ domain and the ligand C terminus. This result suggests that specific residues within the PDZ domains might also influence important functions that are independent of ligand binding and demonstrates the potential of our technique for identifying novel elements important for PSD-95 scaffold function.

These data, together with our analysis of various PSD-95 deletion constructs in this assay, suggest that the PDZ domains of PSD-95 influence complex formation in multiple ways: not only are they responsible for direct interactions with ligand C termini, they also influence the binding of PSD-95 molecules to each other and thereby modulate multimeric complex formation. Using classical methods to analyze the underlying mechanism by which PDZ domains mediate how PSD-95 molecules interact with each other, we provide evidence that PSD-95 multimerization is facilitated by effective ligand binding to PDZ domains, which seems initially to contradict other theories, e.g., that the N-terminal region is the essential requirement for PSD-95 multimerization (Christopherson et al., 2003; Hsueh et al., 1997; Hsueh and Sheng, 1999). Importantly, with the

conditions established for our coIP experiments, we observe only negligible interaction of wild-type PSD-95 molecules with each other; our system, therefore, is not suitable for analysis of N-terminal mutants that potentially hinder multimer formation, which was the basis of earlier studies. Instead, we have established conditions that enable identification of external factors that promote multimerization, and our coIP data indicate a role for ligand binding to PDZ domains in this process. It is important to recognize that all overexpression strategies are limited in that they are suitable only for making direct comparisons between mutant and wild-type recombinant proteins to answer specific questions; however, data from such comparative studies very often has direct application. It is certainly plausible that both of these phenomena, namely the N-terminal interactions described previously and the PDZ domain-mediated effects on PSD-95 behavior that we demonstrate here, play important roles in PSD-95 multimer formation in vivo, and these ideas are the basis of our current work.

In line with our conclusions, a recent study indicated that PDZ-PDZ domain interactions are far more common than previously thought and that they potentially represent a general mechanism underlying scaffold protein multimerization (Chang et al., 2011). Our data suggest that PDZ domains directly facilitate the clustering of multivalent MAGUK scaffold receptor complexes. This occurs through classical PDZ-ligand interactions and also via intermolecular PDZ protein interactions that are, at least in part, mediated directly by the PDZ domains themselves. Such PDZ-PDZ interactions have been studied in more detail for a few individual proteins, namely Shank1 (Im et al., 2003), ZO-1 (Fanning et al., 2007), InaD (Xu et al., 1998), and EBP50/NHERF (Fouassier et al., 2000; Shenolikar et al., 2001). In each of these studies, it is shown that the PDZ domains are capable of dimerization without compromising their ability to bind their ligands via the classical interaction between the C-terminal ligand sequence and the PDZ domain binding groove. There is also some evidence that multimerization of specific PDZ proteins is ligand-dependent and that this regulation may directly involve posttranslational modifications (Lau and Hall, 2001; Maudsley et al., 2000). Such mechanisms may apply to multimerization of PSD-95 molecules; indeed this protein is phosphorylated at multiple sites in neurons and when overexpressed in COS-7 cells (data not shown). This idea ties into the concept of allosteric regulation, namely the idea that alterations at one site of a protein can have effects on the function/activity of the protein at a spatially distinct site. Such mechanisms have established importance for regulation of both transmembrane receptors and enzymatic activity (Taylor et al., 2012; Unal and Karnik, 2012), as well as the function of various scaffold proteins (Zalatan et al., 2012), and recent studies highlight that allosteric regulation is also relevant for other PDZ domain-mediated protein-protein interactions (Gerek and Ozkan, 2011; Reynolds et al., 2011). Of particular relevance for our study, PSD-95 has been investigated in detail with regard to the role of individual amino acids in peptide binding (Gianni et al., 2011; McLaughlin et al., 2012). In these studies, the authors highlight an energetic link between the opposite surfaces of an individual PDZ domain and illustrate the potential for allosteric regulation of PDZ-ligand interactions within the context of the full-length protein.

Also important in the context of our study is data from another group indicating that peptide binding to the PDZ-1 domain of extracytoplasmic heat-shock factor DegP (HtrA) has an allosteric influence on the spatially distinct substrate binding pocket and thereby facilitates protein oligomerization and stabilization of the catalytically active form (Merdanovic et al., 2010). We consider a similar mechanism to explain our observations: binding of the CRIPT C terminus could influence distal surfaces of the third PDZ domain of PSD-95, thus potentially exerting effects on PSD-95 oligomerization via allosteric regulation. In this context, it is especially interesting that binding of CRIPT peptides to PDZ3 of PSD-95 can disrupt a weak but specific intramolecular interaction between PDZ3 and SH3-GK domains (Zhang et al., 2013) and that PSD-95 has been shown to play an important role in the self-assembly of inwardly rectifying Kir2 potassium channel tetrads after binding of individual subunits to individual PSD-95 molecules (Fomina et al., 2011). Structural changes that result from ligand binding could also facilitate the PSD-95 multimer formation observed in our coIP assays. Data from both our coIP experiments and our cell-based ligand clustering split EYFP assay are in line with the idea that allosteric regulation may be an important general mechanism underlying PSD-95 scaffold function: upon binding of ligand C termini to individual PSD-95 molecules, the resulting conformational changes to the PSD-95 molecules promote PSD-95 multimerization and thereby facilitate receptor clustering.

SIGNIFICANCE

Here, we demonstrate that PDZ domains are integral to PSD-95 protein complex formation, and we show that their role in this process extends beyond their function in providing a platform for the binding of ligand C termini. Most importantly, in response to binding of C-terminal ligand sequences to PDZ domains, PSD-95 multimer formation is facilitated, likely due to allosteric effects at distal regions of the PSD-95 molecule. It is plausible that this process also underlies the functional role of PSD-95 at synaptic sites; thus our study provides a basis for future investigations into the role of ligand-dependent MAGUK scaffold formation in postsynaptic receptor clustering.

EXPERIMENTAL PROCEDURES

Constructs

PDZ Scaffolds

Full length rat PSD-95 (NM_019621) was cloned into pCMV-Tag2A and pCMV-Tag3A to obtain N-terminal FLAG and MYC-tagged constructs. Site-directed mutagenesis was used to generate FLAG-PSD-95-D332P, FLAG-PSD-95-R354P, FLAG-PSD-95-V365P, FLAG-PSD-95-L460P, and FLAG-PSD-95-PDZmut (triple mutant: F77H, F172H, F325H) constructs. The short PSD-95 constructs ("MAGUK core") consisting only of the third PDZ domain and the SH3-GK domain were generated by PCR using the respective full length constructs as templates and fragments were cloned into pCMV-Tag2A to generate FLAG-PDZ3-SH3-GK, FLAG-PDZ3-SH3-GK-L460P, and FLAG-PDZ3-SH3-GK-PDZmut constructs. The PSD-95 SH3-GK domain was likewise amplified by PCR and cloned into pCMV-Tag2A to generate the FLAG-PDZ3-SH3-GK construct. A mutant PSD-95 with the two N-terminal cysteines exchanged to serines (C3,5S) and a deleted SH3-GK domain was generated by PCR with a modified N-terminal primer and cloned into pCMV-Tag2A to generate the FLAG-C3,5S-PDZ1-3 construct.

Split-EYFP PDZ Probes

The split-EYFP probe inserts were generated in a two-step PCR. The EYFP split site is located between methionine 154 and alanine 155 of EYFP (…YIM▼ADK…). The first PCR added N-terminal epitope tags (encoded by the forward primers) to the split-EYFP halves and a part of the flexible glycine-serine linker to their C termini (Trinh et al., 2004) (encoded by the reverse primers), pEYFP-N1 (Clontech) served as template. The obtained fragments were gel-purified and used as templates in a second PCR with reverse primers that completed and overlapped with the glycine-serine linker resulting in (3× GGGGS) and encoded the C terminus of the PDZ ligand sequence (ten amino acids). The second PCR was performed with the gel-purified PCR products from the first PCR as templates (YN 1–154 and YC 155–238) together with appropriate forward and reverse primers (HA-YN-for or MYC-YC-for and CRIPT-rev, CRIPTmut-rev, NR2B-rev or NR2Bmut-rev. The resulting eight different PCR products were cloned into pCMV-Tag2A to generate N-terminal HA- or MYC- tagged split EYPF-tagged PDZ probes.

mCherry-CRIPT and mCherry-CRIPTmut

These expression constructs consist of the monomeric red fluorescent protein (mCherry) fused to a glycine-serine linker (3× GGGGS) followed by the ten C-terminal amino acids of a PDZ ligand (CRIPT or CRIPTmut) that corresponds to those in the split-EYFP probes. mCherry-CRIPT and mCherry-CRIPTmut inserts were generated in a two-step PCR as for the split-EYFP probes. Further details including primer sequences are provided in the Supplemental Experimental Procedures.

Cell Culture and Transfection

COS-7 cells were maintained in DMEM containing 10% FCS, PEN-STREP (1,000 U/ml) and 2 mM L-glutamine. The cells were transfected with Lipofectamine 2000 Reagent (Invitrogen) according to the manufacturer's protocol. For clustering assays, each scaffold/split-EYFP PDZ probe combination was transfected in triplicate, and fluorescence was analyzed 20–24 hr posttransfection.

Flow Cytometry and BiFC Assay

Twelve-well plates with transfected COS-7 cells were incubated for 45–60 min at room temperature to promote fluorophore formation. Cells were then harvested by trypsinization and resuspended in PBS/10% FCS for flow cytometry (FL1-530/30 BP filter, BD FACS Calibur). After gating, single-cell events were measured and analyzed for fluorescence (BD CellQuest).

Statistical Analyses

Unless stated otherwise, clustering assays were performed in four independent experiments (in triplicate). For fluorescence quantification of single measurements, 10,000 cells were acquired and analyzed. To combine the results of the four independent experiments, each individual experiment is normalized to an "internal standard" (either PSD-95 + split-EYFP CRIPT probes in Figures 1D, 1F, 3A, 3C, 4B, and 4C, or PDZ3-SH3-GK and split-EYFP CRIPT probes in Figure 5A). Each datapoint (bar) in the results section consist of 12 individual measurements of 10,000 cells each. For every datapoint, the 12 values were tested for Gaussian distribution by D'Agostino and Pearson omnibus normality test. Statistical significance was tested with a two-tailed unpaired t test or 1-way ANOVA/Bonferroni multiple comparison test (GraphPad Prism). Depicted are the mean values ± SD. Degree of significance (as determined by p value calculation) is indicated as follows: *$p < 0.05$; **$p < 0.01$; ***$p < 0.001$; $p > 0.05$ is considered not significant (ns).

Coimmunoprecipitation

Transfected COS-7 cells (one T75 flask) were washed with PBS and harvested 20–24 hr posttransfection with a cell scraper. Cell pellets were resuspended in lysis buffer (50 mM Tris-HCl, 100 mM NaCl, 0.1% NP40, pH 7.5/1 ml per T75 flask) and lysed using a 30-gauge syringe needle. Lysates (1 ml) were cleared by centrifugation and incubated with 2 μg of the appropriate antibody (mouse αHA antibody [Covance], mouse αMYC [Clontech], or normal mouse IgG [Santa Cruz]) for 3 hr followed by a centrifugation at 20,000 × *g*. Supernatants were incubated with 30 μl Protein G-Agarose (Roche) per ml and washed with lysis buffer. Immunocomplexes were collected by centrifugation, denatured, and separated with 12% Tricine-SDS-PAGE (Schägger, 2006). Proteins were blotted onto a PVDF membrane (0.2 μm pore size, Bio-Rad) by semidry transfer (SEMI-DRY TRANSFER CELL, Bio-Rad). Membranes were blocked (PBS, 0.1% Tween 20, 5% dry milk) and incubated overnight with the primary antibody (1:5,000). After incubation with the respective horseradish peroxidase (HRP)-conjugated secondary antibody (1:5,000), blots were visualized using Western Lightning Plus ECL (Perkin Elmer) enhanced chemiluminescence HRP substrate and subsequent film exposure. For detection of additional proteins on the same membranes, blots were incubated in blocking buffer containing sodium azide (0.1%, removing the old HRP signal) together with subsequent primary antibodies as required. The following primary antibodies were used for protein detection: mouse αHA antibody (Covance), rabbit αFLAG (Sigma), mouse αFLAG M2 (Stratagene), goat αGFP (Abcam), rat αTubulin (YL1/2, Abcam), rabbit αDsred (Clontech), and mouse αMYC (Clontech). The following secondary antibodies were used for protein detection: goat αmouse-HRP (Dianova), goat αrabbit-HRP (Dianova), donkey αrabbit-HRP (Santa Cruz), and goat αrat-HRP (Santa Cruz).

Confocal Microscopy

The day prior to transfection, COS-7 cells were seeded on coverslips in 12-well plates. The transfection was carried out using the same conditions as those used for the clustering assay. Twenty-four hours posttransfection, the cells were washed once with PBS and placed upside down onto a glass slide. Images were acquired with a TCS SP5 II laser scanning confocal microscope (Leica).

SUPPLEMENTAL INFORMATION

Supplemental Information includes Supplemental Experimental Procedures and four figures and can be found with this article online at http://dx.doi.org/10.1016/j.chembiol.2013.06.016.

ACKNOWLEDGMENTS

We are grateful Britta Eickholt for critical comments on the manuscript and to Melanie Fuchs for technical assistance. The project was funded by the Deutsche Forschungsgemeinschaft (DFG) (EXC257).

Received: March 1, 2013
Revised: June 11, 2013
Accepted: June 28, 2013
Published: August 22, 2013

REFERENCES

Anderson, J.M. (1996). Cell signalling: MAGUK magic. Curr. Biol. *6*, 382–384.

Chang, B.H., Gujral, T.S., Karp, E.S., BuKhalid, R., Grantcharova, V.P., and MacBeath, G. (2011). A systematic family-wide investigation reveals that ~30% of mammalian PDZ domains engage in PDZ-PDZ interactions. Chem. Biol. *18*, 1143–1152.

Cheng, D., Hoogenraad, C.C., Rush, J., Ramm, E., Schlager, M.A., Duong, D.M., Xu, P., Wijayawardana, S.R., Hanfelt, J., Nakagawa, T., et al. (2006). Relative and absolute quantification of postsynaptic density proteome isolated from rat forebrain and cerebellum. Mol. Cell. Proteomics *5*, 1158–1170.

Cho, K.O., Hunt, C.A., and Kennedy, M.B. (1992). The rat brain postsynaptic density fraction contains a homolog of the Drosophila discs-large tumor suppressor protein. Neuron *9*, 929–942.

Christopherson, K.S., Sweeney, N.T., Craven, S.E., Kang, R., El-Husseini, Ael.-D., and Bredt, D.S. (2003). Lipid- and protein-mediated multimerization of PSD-95: implications for receptor clustering and assembly of synaptic protein networks. J. Cell Sci. *116*, 3213–3219.

Doyle, D.A., Lee, A., Lewis, J., Kim, E., Sheng, M., and MacKinnon, R. (1996). Crystal structures of a complexed and peptide-free membrane protein-binding domain: molecular basis of peptide recognition by PDZ. Cell *85*, 1067–1076.

Ehrlich, I., and Malinow, R. (2004). Postsynaptic density 95 controls AMPA receptor incorporation during long-term potentiation and experience-driven synaptic plasticity. J. Neurosci. *24*, 916–927.

El-Husseini, A.E., Craven, S.E., Chetkovich, D.M., Firestein, B.L., Schnell, E., Aoki, C., and Bredt, D.S. (2000). Dual palmitoylation of PSD-95 mediates its vesiculotubular sorting, postsynaptic targeting, and ion channel clustering. J. Cell Biol. *148*, 159–172.

El-Husseini, Ael.-D., Schnell, E., Dakoji, S., Sweeney, N., Zhou, Q., Prange, O., Gauthier-Campbell, C., Aguilera-Moreno, A., Nicoll, R.A., and Bredt, D.S. (2002). Synaptic strength regulated by palmitate cycling on PSD-95. Cell *108*, 849–863.

Fanning, A.S., Lye, M.F., Anderson, J.M., and Lavie, A. (2007). Domain swapping within PDZ2 is responsible for dimerization of ZO proteins. J. Biol. Chem. *282*, 37710–37716.

Fomina, S., Howard, T.D., Sleator, O.K., Golovanova, M., O'Ryan, L., Leyland, M.L., Grossmann, J.G., Collins, R.F., and Prince, S.M. (2011). Self-directed assembly and clustering of the cytoplasmic domains of inwardly rectifying Kir2.1 potassium channels on association with PSD-95. Biochim. Biophys. Acta *1808*, 2374–2389.

Fouassier, L., Yun, C.C., Fitz, J.G., and Doctor, R.B. (2000). Evidence for ezrin-radixin-moesin-binding phosphoprotein 50 (EBP50) self-association through PDZ-PDZ interactions. J. Biol. Chem. *275*, 25039–25045.

Funke, L., Dakoji, S., and Bredt, D.S. (2005). Membrane-associated guanylate kinases regulate adhesion and plasticity at cell junctions. Annu. Rev. Biochem. *74*, 219–245.

Gerek, Z.N., and Ozkan, S.B. (2011). Change in allosteric network affects binding affinities of PDZ domains: analysis through perturbation response scanning. PLoS Comput. Biol. *7*, e1002154.

Ghosh, I., Hamilton, A.D., and Regan, L. (2000). Antiparallel leucine zipper-directed protein reassembly: application to the green fluorescent protein. J. Am. Chem. Soc. *122*, 5658–5659.

Gianni, S., Haq, S.R., Montemiglio, L.C., Jürgens, M.C., Engström, A., Chi, C.N., Brunori, M., and Jemth, P. (2011). Sequence-specific long range networks in PSD-95/discs large/ZO-1 (PDZ) domains tune their binding selectivity. J. Biol. Chem. *286*, 27167–27175.

Good, M.C., Zalatan, J.G., and Lim, W.A. (2011). Scaffold proteins: hubs for controlling the flow of cellular information. Science *332*, 680–686.

Hsueh, Y.P., and Sheng, M. (1999). Requirement of N-terminal cysteines of PSD-95 for PSD-95 multimerization and ternary complex formation, but not for binding to potassium channel Kv1.4. J. Biol. Chem. *274*, 532–536.

Hsueh, Y.P., Kim, E., and Sheng, M. (1997). Disulfide-linked head-to-head multimerization in the mechanism of ion channel clustering by PSD-95. Neuron *18*, 803–814.

Im, Y.J., Lee, J.H., Park, S.H., Park, S.J., Rho, S.H., Kang, G.B., Kim, E., and Eom, S.H. (2003). Crystal structure of the Shank PDZ-ligand complex reveals a class I PDZ interaction and a novel PDZ-PDZ dimerization. J. Biol. Chem. *278*, 48099–48104.

Kerppola, T.K. (2006). Design and implementation of bimolecular fluorescence complementation (BiFC) assays for the visualization of protein interactions in living cells. Nat. Protoc. *1*, 1278–1286.

Kim, M.J., Futai, K., Jo, J., Hayashi, Y., Cho, K., and Sheng, M. (2007). Synaptic accumulation of PSD-95 and synaptic function regulated by phosphorylation of serine-295 of PSD-95. Neuron *56*, 488–502.

Kornau, H.C., Schenker, L.T., Kennedy, M.B., and Seeburg, P.H. (1995). Domain interaction between NMDA receptor subunits and the postsynaptic density protein PSD-95. Science *269*, 1737–1740.

Lau, A.G., and Hall, R.A. (2001). Oligomerization of NHERF-1 and NHERF-2 PDZ domains: differential regulation by association with receptor carboxyl-termini and by phosphorylation. Biochemistry *40*, 8572–8580.

Lim, I.A., Hall, D.D., and Hell, J.W. (2002). Selectivity and promiscuity of the first and second PDZ domains of PSD-95 and synapse-associated protein 102. J. Biol. Chem. *277*, 21697–21711.

Maudsley, S., Zamah, A.M., Rahman, N., Blitzer, J.T., Luttrell, L.M., Lefkowitz, R.J., and Hall, R.A. (2000). Platelet-derived growth factor receptor association with Na(+)/H(+) exchanger regulatory factor potentiates receptor activity. Mol. Cell. Biol. *20*, 8352–8363.

McCann, J.J., Zheng, L., Rohrbeck, D., Felekyan, S., Kühnemuth, R., Sutton, R.B., Seidel, C.A., and Bowen, M.E. (2012). Supertertiary structure of the synaptic MAGuK scaffold proteins is conserved. Proc. Natl. Acad. Sci. USA *109*, 15775–15780.

McGee, A.W., and Bredt, D.S. (1999). Identification of an intramolecular interaction between the SH3 and guanylate kinase domains of PSD-95. J. Biol. Chem. *274*, 17431–17436.

McGee, A.W., Dakoji, S.R., Olsen, O., Bredt, D.S., Lim, W.A., and Prehoda, K.E. (2001). Structure of the SH3-guanylate kinase module from PSD-95 suggests a mechanism for regulated assembly of MAGUK scaffolding proteins. Mol. Cell *8*, 1291–1301.

McLaughlin, R.N., Jr., Poelwijk, F.J., Raman, A., Gosal, W.S., and Ranganathan, R. (2012). The spatial architecture of protein function and adaptation. Nature *491*, 138–142.

Merdanovic, M., Mamant, N., Meltzer, M., Poepsel, S., Auckenthaler, A., Melgaard, R., Hauske, P., Nagel-Steger, L., Clarke, A.R., Kaiser, M., et al. (2010). Determinants of structural and functional plasticity of a widely conserved protease chaperone complex. Nat. Struct. Mol. Biol. *17*, 837–843.

Nakagawa, T., Futai, K., Lashuel, H.A., Lo, I., Okamoto, K., Walz, T., Hayashi, Y., and Sheng, M. (2004). Quaternary structure, protein dynamics, and synaptic function of SAP97 controlled by L27 domain interactions. Neuron *44*, 453–467.

Niethammer, M., Valtschanoff, J.G., Kapoor, T.M., Allison, D.W., Weinberg, R.J., Craig, A.M., and Sheng, M. (1998). CRIPT, a novel postsynaptic protein that binds to the third PDZ domain of PSD-95/SAP90. Neuron *20*, 693–707.

Okabe, S. (2007). Molecular anatomy of the postsynaptic density. Mol. Cell. Neurosci. *34*, 503–518.

Pan, L., Chen, J., Yu, J., Yu, H., and Zhang, M. (2011). The structure of the PDZ3-SH3-GuK tandem of ZO-1 protein suggests a supramodular organization of the membrane-associated guanylate kinase (MAGUK) family scaffold protein core. J. Biol. Chem. *286*, 40069–40074.

Reese, M.L., Dakoji, S., Bredt, D.S., and Dötsch, V. (2007). The guanylate kinase domain of the MAGUK PSD-95 binds dynamically to a conserved motif in MAP1a. Nat. Struct. Mol. Biol. *14*, 155–163.

Regalado, M.P., Terry-Lorenzo, R.T., Waites, C.L., Garner, C.C., and Malenka, R.C. (2006). Transsynaptic signaling by postsynaptic synapse-associated protein 97. J. Neurosci. *26*, 2343–2357.

Reynolds, K.A., McLaughlin, R.N., and Ranganathan, R. (2011). Hot spots for allosteric regulation on protein surfaces. Cell *147*, 1564–1575.

Schägger, H. (2006). Tricine-SDS-PAGE. Nat. Protoc. *1*, 16–22.

Sheng, M., and Hoogenraad, C.C. (2007). The postsynaptic architecture of excitatory synapses: a more quantitative view. Annu. Rev. Biochem. *76*, 823–847.

Shenolikar, S., Minkoff, C.M., Steplock, D.A., Evangelista, C., Liu, M., and Weinman, E.J. (2001). N-terminal PDZ domain is required for NHERF dimerization. FEBS Lett. *489*, 233–236.

Shin, H., Hsueh, Y.P., Yang, F.C., Kim, E., and Sheng, M. (2000). An intramolecular interaction between Src homology 3 domain and guanylate kinase-like domain required for channel clustering by postsynaptic density-95/SAP90. J. Neurosci. *20*, 3580–3587.

Steiner, P., Higley, M.J., Xu, W., Czervionke, B.L., Malenka, R.C., and Sabatini, B.L. (2008). Destabilization of the postsynaptic density by PSD-95 serine 73 phosphorylation inhibits spine growth and synaptic plasticity. Neuron *60*, 788–802.

Tavares, G.A., Panepucci, E.H., and Brunger, A.T. (2001). Structural characterization of the intramolecular interaction between the SH3 and guanylate kinase domains of PSD-95. Mol. Cell *8*, 1313–1325.

Taylor, S.S., Ilouz, R., Zhang, P., and Kornev, A.P. (2012). Assembly of allosteric macromolecular switches: lessons from PKA. Nat. Rev. Mol. Cell Biol. *13*, 646–658.

Trinh, R., Gurbaxani, B., Morrison, S.L., and Seyfzadeh, M. (2004). Optimization of codon pair use within the (GGGGS)3 linker sequence results in enhanced protein expression. Mol. Immunol. *40*, 717–722.

Unal, H., and Karnik, S.S. (2012). Domain coupling in GPCRs: the engine for induced conformational changes. Trends Pharmacol. Sci. *33*, 79–88.

Xu, X.Z., Choudhury, A., Li, X., and Montell, C. (1998). Coordination of an array of signaling proteins through homo- and heteromeric interactions between PDZ domains and target proteins. J. Cell Biol. *142*, 545–555.

Zalatan, J.G., Coyle, S.M., Rajan, S., Sidhu, S.S., and Lim, W.A. (2012). Conformational control of the Ste5 scaffold protein insulates against MAP kinase misactivation. Science *337*, 1218–1222.

Zhang, P., and Lisman, J.E. (2012). Activity-dependent regulation of synaptic strength by PSD-95 in CA1 neurons. J. Neurophysiol. *107*, 1058–1066.

Zhang, J., Lewis, S.M., Kuhlman, B., and Lee, A.L. (2013). Supertertiary structure of the MAGUK core from PSD-95. Structure *21*, 402–413.

Zheng, C.Y., Petralia, R.S., Wang, Y.X., Kachar, B., and Wenthold, R.J. (2010). SAP102 is a highly mobile MAGUK in spines. J. Neurosci. *30*, 4757–4766.

